Proceedings of the 19th National Conference on Superconductivity, Bronisławów, Poland, October 6–11, 2019

Phonon-Induced Superconducting State: From Metallic Hydrogen to LaH_{10}

A.P. Durajski[a], M.W. Jarosik[a], K.P. Kosk-Joniec[b,*], I.A. Wrona[b], M. Kostrzewa[b], K.A. Szewczyk[b] and R. Szczęśniak[a,b]

[a] *Department of Physics, Częstochowa University of Technology, al. Armii Krajowej 19, 42-200 Częstochowa, Poland*
[b] *Division of Theoretical Physics, Institute of Physics, Jan Długosz University in Częstochowa, al. Armii Krajowej 13/15, 42-200 Częstochowa, Poland*

Doi: 10.12693/APhysPolA.138.715 *e-mail: kamila.kosk-joniec@ajd.czest.pl

The work is a brief review of the current state of knowledge about high-pressure superconductors with a high value of critical temperature (T_c). The described results relate to hydrogen-rich superconductors with particular emphasis on well-known hydrogen sulfide compounds and also include newly-discovered lanthanum hydride compounds. Since in the considered systems the superconductivity is phonon-induced, in theoretical predictions the Eliashberg equations formalism has been used, while some of the results were extended by including the results obtained in calculations using the density functional theory method. Theoretical predictions were compared with the results of experiments available in the literature. A holistic view of the latest results may lead the way to discover the superconductivity at room temperature.

topics: high-temperature superconductivity, hydrogen-rich compounds, Eliashberg formalism

1. Introduction

The phenomenon of superconductivity, observed for the first time in 1911 by Heike Kamerlingh-Onnes, consists in the total disappearance of electrical resistance and appearance of zero induction of the magnetic field in a material cooled below a certain characteristic temperature, called the critical temperature (T_c). This discovery is now considered to be one of the most important findings in the history of physics. The first microscopic theory providing a proper description of the superconductivity phenomenon observed in metals such as Pb, Hg, Sn, Nb and their alloys was BCS theory proposed in 1957 by Bardeen, Cooper and Schrieffer [1, 2]. The basis of this theory is an assumption that below critical temperature electrons couple (the so-called Cooper pairs), creating a superconductive condensate. Generally, since the 1980s, BCS theory has been regarded as the basic theory of superconductivity. A new period of research in superconductivity began in 1986 with the discovery of ceramic superconductors synthesized on the basis of copper oxides [3]. These materials were characterized by substantially higher critical temperatures than those of the conventional superconductors with the electron–phonon pairing mechanism. Unfortunately, there arose a serious problem concerning a proper description of thermodynamics and electrodynamics of their superconductivity within the classic BCS model. It turns out that nowadays there is no complete, generally accepted theory that would explain the pairing mechanism in these systems and show the path of further search for materials that could be superconductors at room temperature [4, 5]. If critical temperature could be raised to the level at which superconductors could be cooled with the help of cheaper solutions than liquid helium or nitrogen, it would undoubtedly lead to a revolution and a huge technological breakthrough, similar to discovering electricity or constructing a computer. It is one of the reasons why wide-ranging research in this field has been conducted for over 100 years.

The main aim of scientific research conducted in this work was a theoretical analysis of high-temperature superconductivity induced by an interaction of electrons with a crystal lattice. Particularly, it focused on selected physical systems in which hydrogen plays a key role in the process of reaching zero resistance in a higher temperature than the boiling temperature of liquid nitrogen (77 K).

In 1968, Ashcroft for the first time paid attention to the possibility of inducing high-temperature superconductivity in metallic hydrogen under high pressure [6]. Recently, this trend in research has been extremely popular which resulted in numerous theoretical papers [7–11]. Unfortunately, due to limited equipment capabilities, the existence of

superconductivity in hydrogen has not been proven experimentally till today. Although the year 2017 saw the publication of an experimental paper on hydrogen metallization around the pressure of 500 GPa [12], these results were severely criticized by the scientific community which means they cannot be treated as credible enough [13, 14]. It might finally turn out that superconductivity in hydrogen does not exist at all but this requires performing some more precise observations.

On the basis of his previous research on superconductivity, Ashcroft predicted in 2004 that introducing hydrogen into a crystal lattice of heavier elements would lead to chemical precompression [15] which would substantially lower the pressure value of metallizing such a system in comparison to the pressure required to metallize pure hydrogen. At the same time, Ashcroft suggested that we can expect superconductivity in such a type of materials to occur at a high value of critical temperature and within pressure values obtained in laboratories. Numerous theoretical research papers [16–20] confirmed the above mentioned predictions which inspired further experiments. The results obtained by Li et al. [17] deserve our special attention since they conducted a wide-ranging structural research on the compound H_2S within the pressure values of $\approx$ 10–200 GPa. The obtained results showed that a growing compression leads to the following series of structural changes: $Pbcm \rightarrow P2/c \rightarrow Pc \rightarrow Pmc2_1$ respectively for pressures of 8.7 GPa, 29 GPa and 65 GPa. It is worth considering the fact that the obtained theoretical results comply with previous experimental data obtained with the use of the X-ray diffraction (XRD) [21, 22]. Two last structural changes occur at the pressure of 80 GPa ($Pmc2_1 \rightarrow P$-1) and 160 GPa (P-1 $\rightarrow Cmca$). Interestingly, the results obtained in [17] contravene previous theoretical prognoses suggesting that H_2S dissociates into sulphur and hydrogen at high pressure [23]. However, it should be noted that a partial dissociation of H_2S was observed above 27 GPa during research conducted with the use of the Raman spectroscopy [24] and XRD [25] at room temperature. The calculations of the electronic structure performed in [17] clearly suggest that the compound H_2S is an insulator till the pressure value of 130 GPa. This result correlates quite well with the value of metallization pressure equalling about 96 GPa, determined experimentally [26]. What is more, Li et al. proved that within the pressure range of 130 to 180 GPa, the compound H_2S shows the existence of superconductivity with the maximum critical temperature of $\approx$ 80 K.

In December 2014, the first experimental results [27] were presented (updated in June 2015 [28] and confirmed in May 2016 [29]) which show that the sample H_2S prepared at low temperature $T < 100$ K and compressed to high pressure obtained in a diamond anvil cell (DAC) has high

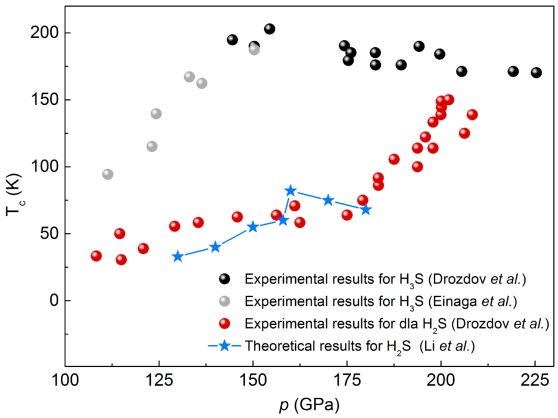

Fig. 1. Critical temperature as a function of pressure for the sample of H_2S prepared at low temperature (red balls) and the sample prepared at room temperature which, due to pressure, was subject to dissociation and formation of H_3S (grey and black balls) [28, 29]. Theoretical results come from the research [17].

values of critical temperature. Especially when it comes to the pressure range from 115 to 200 GPa, T_c rises from 31 to 150 K [28]. As it was shown in Fig. 1, the experimental results correlate very well with theoretical predictions of Li et al. [17]. Interestingly, the sample prepared at room temperature, above the pressure of 43 GPa, is subject to dissociation of the original compound according to the following scheme: $3H_2S \rightarrow 2H_3S+S$ [30–32]. In a newly formed system H_3S, under the pressure of 150 GPa, superconductivity is induced at critical temperature of 203 K. Moreover, one should emphasise the fact that for H_3S a strong isotope effect coming from hydrogen was observed which clearly suggests the electron–phonon character of superconductivity. From the physical point of view, the obtained result means that a superconductor of the highest value of critical temperature known so far has been discovered. Thus, the experimental results discussed can be regarded as groundbreaking from the point of view of research on widely-comprehended high-temperature superconductivity.

In the light of the experimental facts above and theoretical data, a natural direction of the scientific research was expanding knowledge about superconductivity in the family of compounds H_2S and H_3S, twin systems of H_3Cl and H_3P and the mixture $H_3S_{1-x}P_x$. First and foremost, researchers have been looking for a way to raise the value of critical temperature in those systems and get as close as possible to room temperature.

2. The model

From the physical point of view, the description of superconductivity of the compounds in question is based on the idea proposed by Fröhlich [33, 34]. This idea relies on the interaction of electron gas

with the vibrations of a crystal lattice which, within the framework of second quantization, can be modelled with the following statistical operator [35]:

$$H = H^{(0)} + H^{(1)}, \tag{1}$$

where

$$H^{(0)} = \sum_{j\boldsymbol{k}\sigma} \overline{\varepsilon}_{j\boldsymbol{k}} c^{\dagger}_{j\boldsymbol{k}\sigma} c_{j\boldsymbol{k}\sigma} + \sum_{\nu\boldsymbol{q}} \omega_{\nu\boldsymbol{q}} b^{\dagger}_{\nu\boldsymbol{q}} b_{\nu\boldsymbol{q}}, \tag{2}$$

$$H^{(1)} = \frac{1}{\sqrt{N}} \sum_{jl\nu} \sum_{\boldsymbol{k}\boldsymbol{q}\neq 0,\sigma} g_{\nu}^{j\boldsymbol{k}+\boldsymbol{q},l\boldsymbol{k}}(\boldsymbol{q}) \times c^{\dagger}_{j\boldsymbol{k}+\boldsymbol{q}\sigma} c_{l\boldsymbol{k}\sigma} \left(b_{\nu\boldsymbol{q}} + b^{\dagger}_{\nu-\boldsymbol{q}} \right). \tag{3}$$

The values $c^{\dagger}_{j\boldsymbol{k}\sigma}$ and $c_{j\boldsymbol{k}\sigma}$ are accordingly the operator of creation and annihilation of the electron state in j-band at momentum $\boldsymbol{k}$ and spin $\sigma \in \{\uparrow, \downarrow\}$. Symbol $\overline{\varepsilon}_{j\boldsymbol{k}}$ is defined by the formula: $\overline{\varepsilon}_{j\boldsymbol{k}} = \varepsilon_{j\boldsymbol{k}} - \mu$, where $\varepsilon_{j\boldsymbol{k}}$ is the band energy of electrons and μ signifies the chemical potential. Accordingly, $b^{\dagger}_{\nu\boldsymbol{q}}$ and $b_{\nu\boldsymbol{q}}$ represent the operator of creation and annihilation of a phonon in a mode ν and momentum $\boldsymbol{q}$ and $\omega_{\nu\boldsymbol{q}}$ determines the value of phonon energy. The energy of electron–phonon interaction is expressed by $g_{\nu}^{j\boldsymbol{k}+\boldsymbol{q},l\boldsymbol{k}}(\boldsymbol{q})$.

Eliminating phonon degrees of freedom, with the help of a canonical transformation, from the above statistical operator we get a Hamiltonian of BCS theory which can be subsequently analysed within the framework of the mean-field approximation. Unfortunately, this approach does not allow for a quantitative description of superconductivity of the systems in which the value of electron–phonon coupling λ is $\gtrapprox 0.5$ (a conventional limit of weak coupling). In most hydrogenated superconductors, we deal with strong $\lambda > 1$ or very strong $\lambda > 2$ electron interaction with the crystal lattice. The compounds such as SiH_4, SnH_4 and H_2S would belong to the first group [17, 36, 37]. On the other hand, the systems characterized by very strong electron–phonon coupling are among others CaH_6, YH_6, YH_{10}, SrH_{10} and H_3S [20, 36, 37]. Considering the facts above, our analysis of thermodynamic properties of the above mentioned materials was based on the formalism of the Eliashberg equations [38] constituting the generalization of BCS theory for the systems characterized by the strong electron–phonon coupling [39]. Contrary to BCS theory, the results obtained within the framework of the Eliashberg formalism, at their quantitative level, comply with experimental measurements, regardless of the fact whether the analysed system is characterized by a strong or weak electron–phonon coupling. There are even some premises saying that the Eliashberg formalism might be used for the analysis of thermodynamic properties of high-temperature oxygen–copper superconductors [40, 41].

In order to develop the Eliashberg system of equations, firstly one should write the operator (1) in a matrix notation with the use of the Nambu spinor [42]. Next, to obtain a Dyson-type equation [43], a Matsubara–Green function is defined [44], where diagonal elements describe thermodynamic properties of normal state above the critical temperature and non-diagonal elements characterize superconductivity [45]. In the last calculation stage, the procedure of self-consistent procedure for the formula of self-energy is used.

In the case of superconductors with wide energy bands, such as hydrogenated compounds under high pressure, the Eliashberg system of equations for the function of the order parameter $\varphi_n = \varphi(\mathrm{i}\omega_n)$ and the wave function renormalization factor $Z_n = Z(\mathrm{i}\omega_n)$ takes the following form (one-band, isotropic version):

$$\varphi_n = \pi T \sum_{m=-M}^{M} \frac{\Lambda_{n,m} - \mu^{\star}\theta(\omega_c - |\omega_m|)}{\sqrt{(\omega_m Z_m)^2 + \varphi_m^2}} \varphi_m, \tag{4}$$

$$Z_n = 1 + \frac{\pi T}{\omega_n} \sum_{m=-M}^{M} \frac{\Lambda_{n,m}}{\sqrt{(\omega_m Z_m)^2 + \varphi_m^2}} \omega_m Z_m, \tag{5}$$

where ω_n is the n-th fermionic Matsubara frequency $\omega_n = \pi(2n-1)/\beta$, and θ is the Heaviside step function, whereas ω_c signifies the cut-off frequency. Conventionally, it is assumed that the value of ω_c falls within the range from $3\omega_{\mathrm{D}}$ to $10\omega_{\mathrm{D}}$, where ω_{D} is the Debye frequency [46]. Its value, in the case of analysed hydrogenated systems, falls within the range from 200 to 350 meV, depending on the value of the applied pressure. The pairing kernel for electron–phonon interaction is defined in the following way:

$$\Lambda_{n,m} = 2 \int_0^{\omega_{\mathrm{D}}} \mathrm{d}\omega \frac{\omega \alpha^2 F(\omega)}{\omega^2 + (\omega_n - \omega_m)^2}. \tag{6}$$

The Eliashberg function, i.e., $\alpha^2 F(\omega)$, being one of two input elements for Eliashberg equations, plays the role of a bridge between theory and experiment. It is calculated most often with the help of quantum-mechanical (DFT) methods [47–49]. It can also be determined experimentally in the tunnel experiment [50, 51] or with the use of the angle-resolved photoemission spectroscopy (ARPES) method [52]. From the theoretical point of view, an experimental approach is crucial as it ensures the possibility of direct comparison of the obtained experimental and numerical results which constitutes a test for the accuracy of theoretical calculations [53]. In the Eliashberg formalism, in the situation where the experimental value of T_c is known, the Coulomb pseudopotential $\mu^{\star}$ (the second input element for the Eliashberg equations) modelling decoupling interaction between electrons is selected so that critical temperature obtained from the numerical analysis complies with its value obtained from experimental calculations. If there are no experimental data, an approximate value of the parameter $\mu^{\star}$ can be assessed with the help of the Morel–Anderson formula [54, 55]:

$$\mu^{\star} = \frac{\mu}{1 + \mu \ln(\varepsilon_{\mathrm{F}}/\omega_{\ln})}, \tag{7}$$

where $\mu = \rho(\varepsilon_{\mathrm{F}})\, U_c$. The symbol U_c represents the Coulomb potential and $\rho(\varepsilon_{\mathrm{F}})$ signifies the density of states (DOS) at the Fermi level ε_{F}. The symbol $\omega_{\ln}$ signifies the logarithmic frequency of the form

$$\omega_{\ln} = \exp\left(\frac{2}{\lambda}\int_0^{\omega_{\mathrm{D}}} \mathrm{d}\omega \frac{\ln(\omega)\,\alpha^2 F(\omega)}{\omega}\right). \tag{8}$$

Professional literature usually accepts the value between 0.1 and 0.2 for the parameter $\mu^\star$. It can be proven in a relatively simple way that the assumption is correct in the case of the investigated hydrogenated compounds. Let us note that the maximum value of $\mu^\star$ can be defined once it is assumed that $\mu \to +\infty$ (the limit of infinite U_c) which lets us write (7) in the following form [55]:

$$\mu^\star_{\max} = \frac{1}{\ln(\varepsilon_{\mathrm{F}}/\omega_{\ln})}. \tag{9}$$

For example, for the compound of H_3S under the pressure of 200 GPa, we get $\varepsilon_{\mathrm{F}} = 17.506$ meV and $\omega_{\ln} = 131$ meV [56] which gives us a result $\mu^\star_{\max} \approx 0.2$. Additionally, the paper [56] confirms that the above mentioned result complies with the estimate of the critical value of $\mu^\star$ obtained with the help of the Eliashberg equations, on the basis of providing the experimental value of critical temperature ($\mu^\star_{\mathrm{c}} = 0.204$).

Taking a broader view on the issue, one should pay attention to the fact that $\varepsilon_{\mathrm{F}} \gg \omega_{\ln}$, thus within the Morel–Anderson approach implemented, the value of the Coulomb pseudopotential usually is 0.1–0.2 and $\mu^\star \ll \mu$. The above result creates a certain problem as in many cases high-pressure superconductivity is characterised by $\mu^\star \geq 0.3$. This situation occurs, for example, in lithium where the Coulomb pseudopotential rises together with pressure increase till the value of 0.36 for $p = 29.7$ GPa [57]. This issue was solved by Bauer, Han and Gunnarsson who made calculations up to second order in U_c [58]. On the basis of these calculations, they stated that retardation effects lead to the decrease in the value of $\mu \to \mu^\star$, however, it is not as significant as in the case of Morel–Anderson formula. In the case in question, the following formula was obtained:

$$\mu^\star = \frac{\mu + a\mu^2}{1 + \mu\ln\left(\frac{\varepsilon_F}{\omega_{\ln}}\right) + a\mu^2\ln\left(\alpha\frac{\varepsilon_F}{\omega_{\ln}}\right)}, \tag{10}$$

where the constant $a = 1.38$ and $\alpha \simeq 0.10$. Within the range of infinite U_c, one can obtain

$$\mu^\star_{\max} = \frac{1}{\ln\left(\alpha\frac{\varepsilon_{\mathrm{F}}}{\omega_{\ln}}\right)}. \tag{11}$$

In the case of H_3S, the value of the Coulomb pseudopotential obtained with the help of the formula above ($\mu^\star_{\max} \approx 0.38$) is clearly too high in relation to numerical analyses. Nevertheless, the analysis performed for H_5S_2 shows that in extreme cases for hydrogenated compounds $\mu^\star$ can take bigger values than 0.4 [59].

During the conducted research, we solved the Eliashberg equations on an imaginary axis and in mixed representation (the equations defined simultaneously on the imaginary axis and the real one). We used iterative methods described, e.g., in [60]. In particular, the equations defined on the imaginary axis let us determine quantitatively the value of critical temperature, the difference of free energy between normal and superconductive states, thermodynamic critical field, specific heat for superconductivity and estimate values for a band gap at the Fermi level and electron effective mass. The exact values of the two last parameters were determined with the help of the Eliashberg equations in mixed representation [46, 61]:

$$\begin{aligned}\varphi(\omega + \mathrm{i}\delta) = {} & \frac{\pi}{\beta}\sum_{m=-M}^{M}\frac{\varphi_m}{\sqrt{(\omega_m Z_m)^2 + \varphi_m^2}}\left[\lambda(\omega - \mathrm{i}\omega_m) - \mu^\star\theta(\omega_c - |\omega_m|)\right] \\ & + \mathrm{i}\pi\int_0^{+\infty}\mathrm{d}\omega'\alpha^2F(\omega')\left[\Big(N(\omega') + f(\omega' - \omega)\Big)\frac{\varphi(\omega - \omega' + \mathrm{i}\delta)}{\sqrt{(\omega - \omega')^2 Z^2(\omega - \omega' + \mathrm{i}\delta) - \varphi^2(\omega - \omega' + \mathrm{i}\delta)}}\right] \\ & + \mathrm{i}\pi\int_0^{+\infty}\mathrm{d}\omega'\alpha^2F(\omega')\left[\Big(N(\omega') + f(\omega' + \omega)\Big)\frac{\varphi(\omega + \omega' + \mathrm{i}\delta)}{\sqrt{(\omega + \omega')^2 Z^2(\omega + \omega' + \mathrm{i}\delta) - \varphi^2(\omega + \omega' + \mathrm{i}\delta)}}\right]\end{aligned} \tag{12}$$

and

$$\begin{aligned}Z(\omega + \mathrm{i}\delta) = {} & 1 + \frac{\mathrm{i}\pi}{\omega\beta}\sum_{m=-M}^{M}\frac{\lambda(\omega - \mathrm{i}\omega_m)\omega_m Z_m}{\sqrt{(\omega_m Z_m)^2 + \varphi^2}} \\ & + \frac{\mathrm{i}\pi}{\omega}\int_0^{+\infty}\mathrm{d}\omega'\alpha^2F(\omega')\left[\Big(N(\omega') + f(\omega' - \omega)\Big)\frac{(\omega - \omega')Z(\omega - \omega' + \mathrm{i}\delta)}{\sqrt{(\omega - \omega')^2 Z^2(\omega - \omega' + \mathrm{i}\delta) - \varphi^2(\omega - \omega' + \mathrm{i}\delta)}}\right] \\ & + \frac{\mathrm{i}\pi}{\omega}\int_0^{+\infty}\mathrm{d}\omega'\alpha^2F(\omega')\left[\Big(N(\omega') + f(\omega' + \omega)\Big)\frac{(\omega + \omega')Z(\omega + \omega' + \mathrm{i}\delta)}{\sqrt{(\omega + \omega')^2 Z^2(\omega + \omega' + \mathrm{i}\delta) - \varphi^2(\omega + \omega' + \mathrm{i}\delta)}}\right],\end{aligned} \tag{13}$$

where the symbols $N(\omega)$ and $f(\omega)$ mean the Bose–Einstein and the Fermi–Dirac distribution accordingly

$$N(\omega) = \frac{1}{\mathrm{e}^{\beta\omega} - 1} \quad \text{and} \quad f(\omega) = \frac{1}{\mathrm{e}^{\beta\omega} + 1}. \tag{14}$$

3. Superconductivity in hydrogen sulfide compounds

The discovery of a very high value of critical temperature, especially exceeding 200 K in hydrogen sulfide compounds, was a kind of breakthrough in the superconductivity research. This fact resulted in an incredible increase in interest of scientists in this group of superconductors associated with the hope of further increase of T_c value. First, extensive research was needed to fully understand the properties of these superconductors.

In the first step, we have analysed the system of H_2S under the influence of pressure from the range of 130 to 180 GPa [62]. For the value of the Coulomb pseudopotential equalling 0.15, we have reconstructed the experimental dependence of critical temperature on pressure, $T_c \in \langle 31, 88 \rangle$ K, and we have determined other crucial thermodynamic values of superconductivity, such as the band gap on the Fermi surface, the specific heat and the thermodynamic critical field. Due to the strong electron–phonon coupling and retardation effects, the results obtained substantially differ from predictions of classical BCS theory. By generalising the obtained results, we have estimated the maximum value of critical temperature possible to be observed in compounds of H_nS type, where $n = 1,\ 2,\ 3$. In the beginning, we noticed that the contributions for the Eliashberg function coming from sulphur and hydrogen are most clearly separated. In particular, in the range of low frequency, the electron–phonon interaction coming from sulphur is crucial, whereas for higher frequencies the contribution of hydrogen becomes important [17]. The situation in question is illustrated in Fig. 2 which presents the results for the pressure of 160 GPa at which Li et al. [17] note the highest critical temperature equalling ≈ 80 K.

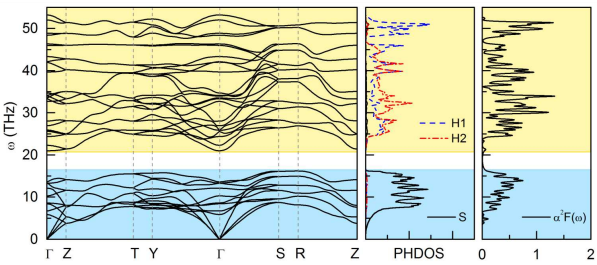

Fig. 2. Phonon spectrum, phonon density of states (PhDOS) and the Eliashberg function $\alpha^2 F(\omega)$ for H_2S under the pressure of 160 GPa [17].

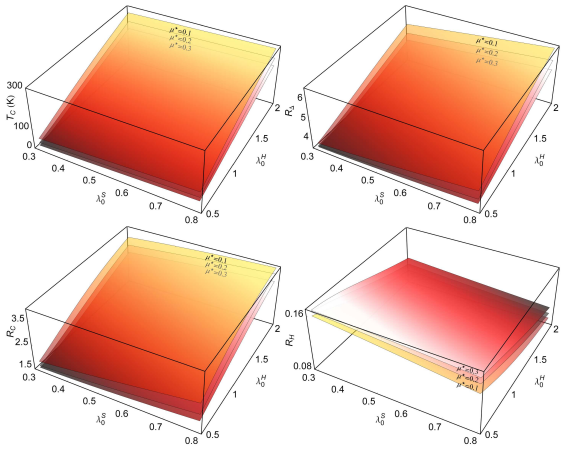

Fig. 3. Critical temperature and non-dimensional parameters R_Δ, R_c and R_h in the function of the coupling constant λ_0^{S} and λ_0^{H} for selected values of the Coulomb pseudopotential [62].

Taking into account the above fact, a model Eliashberg function can be written as follows:

$$\alpha^2 F(\omega) = \lambda_0^{\mathrm{S}} \left(\frac{\omega}{\omega_{\max}^{\mathrm{S}}} \right)^2 \theta\left(\omega_{\max}^{\mathrm{S}} - \omega\right) + \lambda_0^{\mathrm{H}} \left(\frac{\omega}{\omega_{\max}^{\mathrm{H}}} \right)^2 \theta\left(\omega_{\max}^{\mathrm{H}} - \omega\right), \tag{15}$$

where λ_0^{S} and λ_0^{H} constitute input for the constant of electron–phonon coupling, from sulphur and hydrogen accordingly. Furthermore, the symbols $\omega_{\max}^{\mathrm{S}}$ and $\omega_{\max}^{\mathrm{H}}$ signify the maximum phonon frequencies. On the basis of the previous research, the following input parameters have been assumed: $\lambda_0^{\mathrm{S}} \in \langle 0.3,\ 0.8 \rangle$ and $\omega_{\max}^{\mathrm{S}} = 70$ meV [63], and $\lambda_0^{\mathrm{H}} \in \langle 0.5,\ 2.0 \rangle$ and $\omega_{\max}^{\mathrm{H}} = 220$ meV [8].

As a result of the analysis performed, it was found out that the maximum value of critical temperature for $\mu^\star = 0.1$ equals 290 K. It should be emphasised that the Coulomb pseudopotential taken for the calculations complies with the estimation performed in Ashcroft's fundamental publication [15]. From the physical point of view, the obtained value T_c constitutes a very important result as it shows that there is a real possibility to achieve superconductivity at critical temperature close to room temperature. This result is always a direct motivation for further research aiming at finding a way to raise T_c.

In a similar way, non-dimensional parameters linked with the band gap, specific heat and thermodynamic critical field have been determined: $R_\Delta = 2\Delta(0)/k_{\mathrm{B}}T_c$, $R_c = \Delta C(T_c)/C^N(T_c)$ and $R_h = T_c C^N(T_c)/H_c^2(0)$. It should be noted that the relations above, within classic BCS theory, take universal values: $R_\Delta = 3.53$, $R_c = 1.43$ and $R_h = 0.168$.

In the case of H_nS compounds, the maximum values of the parameters R_Δ and R_c and the minimum value of the parameter R_h clearly diverge from

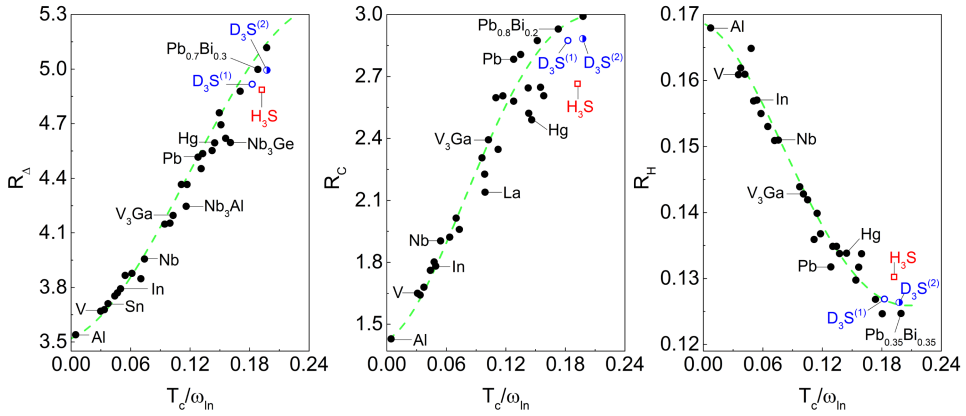

Fig. 4. Non-dimensional parameters R_Δ, R_c and R_h in the function of $T_c/\omega_{\ln}$. Experimental points taken from [39]. The results for $D_3S^{(1)}$ and $D_3S^{(2)}$ correspond to critical temperature which equals 147 K and 159 K [68].

classic BCS theory and equal 6.53, 3.99 and 0.093, respectively. The complete results in the function of the constant of the coupling λ_0^{S} and λ_0^{H} for selected values of the Coulomb pseudopotential are gathered in Fig. 3. The presented results, and in particular those for T_c, suggest that it is possible to obtain superconductivity at room temperature in the family of hydrogenated compounds built on the basis of sulphur. This conclusion led to the publications of [64–67] which analyse selected options that might lead to obtaining a critical temperature higher than 203 K.

Next important results were presented in the publication [68] where a detailed analysis of H_3S compound and its isotope counterpart D_3S have been conducted. Based on spectral functions determined in [69], for the pressure of 150 GPa, the experimental value of critical temperature equalling 203 K for H_3S and 147 K for D_3S were reconstructed. What is more, the work thoroughly discussed the fact of change in the value of isotope coefficient α together with pressure. For pure metals, there is a relation $T_c M^\alpha = \text{const}$, where M is the atomic mass of the isotope contained in the lattice structure of the superconductor and the exponent α approximately equals 0.5 [70]. On this basis, the exponent α can be described for the compounds analysed by

$$\alpha = -\frac{\ln(T_c)_{\mathrm{D_3S}} - \ln(T_c)_{\mathrm{H_3S}}}{\ln(M)_{\mathrm{D}} - \ln(M)_{\mathrm{H}}}, \tag{16}$$

where $(T_c)_{\mathrm{H_3S}}$ ($(T_c)_{\mathrm{D_3S}}$) is the critical temperature of the hydrogen (deuterium)-based system and $(M)_{\mathrm{H}}$ ($(M)_{\mathrm{D}}$) is the hydrogen (deuterium) atomic mass.

In the publication in question, on the basis of linear matching of experimental data $T_c(p)$ for H_3S and D_3S and by analysing the value of the Coulomb pseudopotential with the help of the Morel–Anderson formula [54, 55], it was suggested that the experimental value of T_c for D_3S is underestimated and should really equal about 159 K which would allow for achieving the value of α equalling 0.35 (the value observed under higher pressure from 170 to 220 GPa). Otherwise, the coefficient in question is 0.47. Moreover, thermodynamic properties of the analysed systems were compared to properties of other conventional superconductors. It turned out that regardless of substantial deviations from BCS theory predictions, H_3S and D_3S compounds ideally match the trend set by other conventional superconductors. It is illustrated in Fig. 4 by the overview of the non-dimensional parameters obtained R_Δ, R_c and R_h in the function of $T_c/\omega_{\ln}$.

The validity of applying classical formalism of the Eliashberg equations for the description of hydrogenated compounds was confirmed in [56] with the analysis of the influence of a lowest-order vertex correction for the electron–phonon interaction on superconductivity in H_3S and its twin system H_3P for which the experimental results confirm the occurrence of a superconductive phase below the temperature of 103 K [71]. In particular, using the density functional theory (DFT) methods implemented in Quantum-ESPRESSO software, the electron and phonon properties of the compounds in question were determined and the Eliashberg functions were defined as follows [47, 48]:

$$\alpha^2 F(\omega) = \frac{1}{2\pi\rho(\varepsilon_{\mathrm{F}})} \sum_{\nu \boldsymbol{q}} \frac{\gamma_{\nu \boldsymbol{q}}}{\omega_{\nu \boldsymbol{q}}} \delta(\omega - \omega_{\nu \boldsymbol{q}}), \tag{17}$$

where the symbol $\gamma_{\nu \boldsymbol{q}}$ defines the width of phonon lines:

$$\gamma_{\nu \boldsymbol{q}} = 2\pi\omega_{\nu \boldsymbol{q}} \sum_{ij} \int \frac{\mathrm{d}^3 k}{\Omega_{\mathrm{BZ}}} \left| g_\nu^{j\boldsymbol{k}+\boldsymbol{q}, l\boldsymbol{k}}(\boldsymbol{q}) \right|^2$$

$$\times \delta(\varepsilon_{i\boldsymbol{q}} - \varepsilon_{\mathrm{F}}) \delta(\varepsilon_{j\boldsymbol{k}+\boldsymbol{q}} - \varepsilon_{\mathrm{F}}). \tag{18}$$

Then, on the basis of the determined functions $\alpha^2 F(\omega)$ for the pressure of 200 GPa, the experimental values of critical temperature (178 K for H_3S and 81 K for H_3P) have been reconstructed using classic Eliashberg equations and extended equations complemented by vertex corrections which take the following form [72, 73]:

$$\varphi_n = \pi T \sum_{m=-M}^{M} \frac{\Lambda_{n,m} - \mu^\star \theta\left(\omega_c - |\omega_m|\right)}{\sqrt{(\omega_m Z_m)^2 + \varphi_m^2}} \varphi_m$$
$$- \frac{\pi^3 T^2}{4\varepsilon_{\mathrm{F}}} \sum_{m=-M}^{M} \sum_{m'=-M}^{M} \frac{\Lambda_{n,m}\Lambda_{n,m'}}{\sqrt{\left(\omega_m Z_m^2 + \varphi_m^2\right)\left(\omega_{m'} Z_{m'}^2 + \varphi_{m'}^2\right)\left(\omega_{-n+m+m'}^2 Z_{-n+m+m'}^2 + \varphi_{-n+m+m'}^2\right)}}$$
$$\times \left(\varphi_m \varphi_{m'} \varphi_{-n+m+m'} - \omega_m Z_m \omega_{m'} Z_{m'} \varphi_{-n+m+m'} + 2\varphi_m \omega_{m'} Z_{m'} \omega_{-n+m+m'} Z_{-n+m+m'}\right) \tag{19}$$

and

$$Z_n = 1 + \frac{\pi T}{\omega_n} \sum_{m=-M}^{M} \frac{\Lambda_{n,m}}{\sqrt{(\omega_m Z_m)^2 + \varphi_m^2}} \omega_m Z_m$$
$$- \frac{\pi^3 T^2}{4\varepsilon_{\mathrm{F}} \omega_n} \sum_{m=-M}^{M} \sum_{m'=-M}^{M} \frac{\Lambda_{n,m}\Lambda_{n,m'}}{\sqrt{\left(\omega_m^2 Z_m^2 + \varphi_m^2\right)\left(\omega_{m'}^2 Z_{m'}^2 + \varphi_{m'}^2\right)\left(\omega_{-n+m+m'}^2 Z_{-n+m+m'}^2 + \varphi_{-n+m+m'}^2\right)}} \tag{20}$$
$$\times \left(\omega_m Z_m \omega_{m'} Z_{m'} \omega_{-n+m+m'} Z_{-n+m+m'} + 2\omega_m Z_m \varphi_{m'} \varphi_{-n+m+m'} - \varphi_m \varphi_{m'} \omega_{-n+m+m'} Z_{-n+m+m'}\right).$$

The obtained results allow to notice a considerable reduction of the Coulomb pseudopotential value, once vertex corrections are taken into account. It is a crucial result as it decreases the contribution of the parameter whose function, in fact, is to match theoretical results to experimental data. However, further analysis showed that regardless of the change in the value of the depairing parameter by -9.3% in the case of H_3S and by -5.7% in the case of H_3P, the course of the order parameter obtained within the framework of the classic Eliashberg equations does not differ from the one obtained with the help of the equations extended by vertex corrections. It means that the thermodynamic properties of the systems in question can be successfully analysed within the classical Migdal–Eliashberg approach provided that the Coulomb pseudopotential is appropriately matched.

Research on the impact of vertex corrections on superconductivity in the compound of H_3S was also carried out by Sano et al. [35]. These studies proved that once the value of $\mu^\star$ is determined beforehand, lowest-order vertex corrections, similarly to anharmonic effects [74], substantially reduce (about 20%) the value of critical temperature. The negative influence of vertex corrections on the value of T_c was also confirmed by the results of research conducted for the compound of H_3Cl [67]. However, it should be noted that the observed reductions amount to merely about 2%. The existence of such big discrepancies derives from the difference in the method of analysing vertex corrections. Our calculations are based on ignoring momentum dependence and solving the Eliashberg equations with vertex correction in a self-consistent way. On the other hand, Sano does not omit momentum dependence but introduces a series of additional approximations and finally does not obtain his result in a self-consistent way. It is worth emphasising that both the first and the second method have their flaws. That is why the best solution would be to introduce and solve complete equations in a self-consistent way. From the mathematical point of view, it is quite a complex issue but worth our attention, like the analysis of high-order vertex corrections.

The next paper [64] presents systematic research which was aimed at obtaining critical temperature close to room temperature. It focused on the increase of pressure as one possible factor allowing for the achievement of the desired effect. External pressure can be regarded as a parameter which allows for controlling the properties of researched materials. A change in pressure leads to a change in the distance between atoms which in some conditions can cause metallization of the system and a transition into the superconductivity state. It also influences the increase of such key values as the constant of the electron–phonon coupling or critical temperature. The best example is calcium which, while exposed to compression, experiences a series of structural transformations while its T_c grows till the value of 29 K which so far has been the highest critical temperature obtained experimentally for an element [75]. In the case of hydrogen, theoretical research suggests that the increase in pressure to an extremely high value of 2000 GPa might cause transition from the normal to superconductive state at the temperature of 600 K [8, 76]. Of course, it is not a rule that a pressure rise causes T_c increase. In certain circumstances, it can lead to T_c decrease and even to a superconductivity loss. Such a situation takes place, for example, in the case of lithium [77] or the compound of MgB_2 [78].

In the light of the information above, it turned out to be very important to check how the system H_3S behaves in conditions of very high pressure. The initial stage of research encompassed the procedure of optimization of lattice constants and atom location in an elementary cell by minimizing the system's enthalpy due to the value of the assumed pressure. With the obtained minimum,

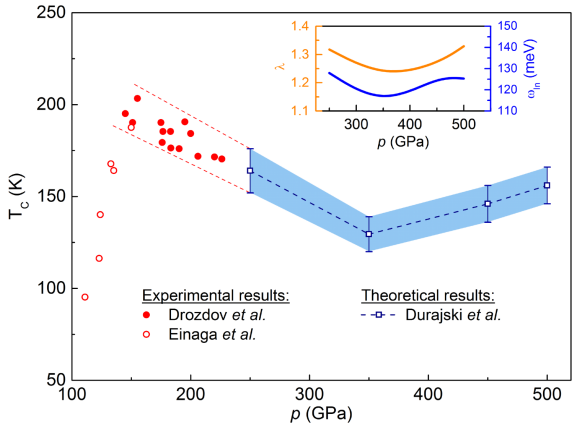

Fig. 5. Critical temperature in the function of pressure for H_3S. Deviations from set values of T_c were obtained for $\mu^\star = 0.11$–0.15 [64].

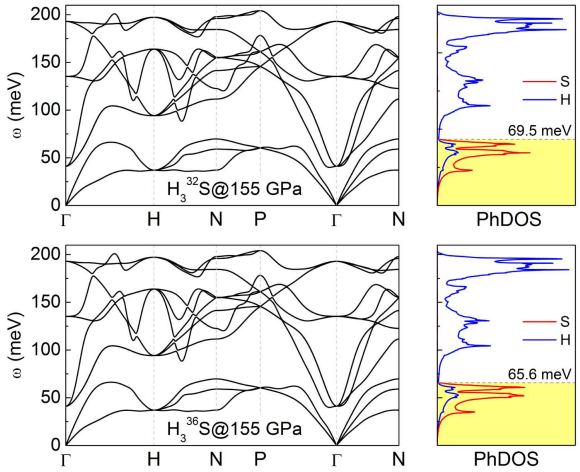

Fig. 6. The influence of sulphur isotope change on the phonon structure of H_3S [65].

further simulations could be made which were then subsequently completed by calculations performed within the frame of the Eliashberg theory. The results show that in the pressure range from 250 to 500 GPa, the system H_3S of lattice structure $Im\overline{3}m$ is dynamically stable. This fact manifests itself in a lack of imaginary frequencies in the phonon spectrum. The enthalpy diagram in the function of pressure also confirms a tendency to keep the cubic structure of the system above the value of 180 GPa. Moreover, for all the pressure values analysed, one can notice a clear maximum in electron density of states near the Fermi surface which, to a large extent, is responsible for inducing high-temperature superconductivity in H_3S [35, 79, 80]. All this analysis leads to the conclusion that increasing pressure to the limits of laboratory possibilities (≈ 500 GPa) does not allow for obtaining the superconductivity state in the compound of H_3S above the temperature of 200 K.

Figure 5 illustrates the course of T_c in the function of pressure. Importantly, the results obtained in the range from 250 to 350 GPa correspond very well to experimental data for lower pressure values, marked in the diagram by red symbols [28, 29]. On the other hand, over 350 GPa, there is an opposite trend and critical temperature begins to rise systematically till its maximum value equalling 155 ± 10 for the pressure of 500 GPa. The described course strongly correlates with the function of the electron–phonon coupling constant

$$\lambda = 2 \int_0^{\omega_D} d\omega \frac{\alpha^2 F(\omega)}{\omega} \tag{21}$$

and the course of the logarithmic phonon frequency (ω_{ln}). The calculated values of λ and ω_{ln} were drawn in the function of pressure in inset of Fig. 5. The results above strongly suggest that experimenters should look for a different method which would allow them to achieve the superconductivity state in room temperature.

Following that research path in [65], we examined the influence of sulphur isotopes on the superconductivity state in H_3S. In the case of replacing hydrogen with deuterium in an elementary cell, the reduction of critical temperature was experimentally proved, whereas, in the case of sulphur, professional literature does not contain any information on this topic. Generally, we can distinguish four stable, naturally occurring sulphur isotopes: ^{32}S (31.972 u), ^{33}S (32.971 u), ^{34}S (33.968 u) and ^{36}S (35.967 u). For all the cases above, numerical analyses have been conducted within the pressure range from 155 to 225 GPa. The pressure range was not chosen at random and it strictly corresponds to the experimental results obtained for the structure $Im\overline{3}m$ which makes it possible to perform a comparative analysis of the results obtained with the experimental data. As it was anticipated, the performed research allowed to conclude that sulphur isotope change does not have any influence on the electron structure of the system analysed. However, there are interesting outcomes in the phonon structure. Increasing mass of the sulphur isotope makes the boundary of the input coming from sulphur shift to the constant of electron–phonon coupling towards lower values which means that the percentage input coming from hydrogen increases.

Figure 6 presents phonon structures and PhDOS for two extreme cases: the isotope with the minimum atomic mass (^{32}S) and the isotope with the maximum atomic mass (^{36}S). The area marked yellow shows the range of frequencies in which vibrations coming from sulphur are of primary importance. Due to the above mentioned shift, we can observe a non-typical isotopic effect reflected in the critical temperature increase to the value of 242 K at the pressure of 155 GPa and the isotope of ^{36}S.

Figure 7 shows detailed results. The value of the Coulomb pseudopotential was matched in such a way as to make it possible to reconstruct

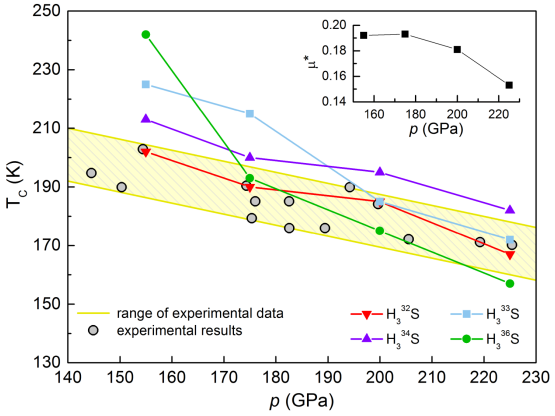

Fig. 7. Critical temperature in the function of pressure for H_3S with different sulphur isotopes [65].

experimental results for the average sulphur mass. Analysing the T_c change graph in the function of pressure, one has to pay attention to the fact that despite reversed and non-trivial isotope effect, a pressure growth is accompanied with a general decrease in critical temperature, in accordance with the trend set by experimental points. The results presented in the work [65] show that the growth in the value of critical temperature by almost 40 K, in relation to a record-like experimental result, is possible. It is one more proof of electron–phonon pairing character in the compounds of hydrogen and sulphur, provided that theoretical results are experimentally proven.

In 2016, a record value of T_c equalling 280 K was predicted in the compound $H_3S_{0.925}P_{0.075}$ [81]. A widely-ranged numerical analysis has been performed in [81], based on the method of virtual crystal approximation (VCA). In this method, in an elementary cell of H_3S, atom S is replaced with a pseudopotential which is a specially constructed superposition of two atoms, S and P in the proportions corresponding to the assumed chemical composition. This method is much more effective than the supercell method as calculations rely on a primitive cell, though in some situations it might turn out much less credible. Analysing in detail the results from [81], one can observe that critical temperature for the system $H_3S_{0.925}P_{0.075}$ grows systematically, together with pressure from the value of 224 ± 18 K for 150 GPa to 260 ± 20 K for 250 GPa. This result goes against the trend set by experimental data for H_3S which show T_c decrease accompanied by pressure growth in the range beyond 150 GPa [27]. Due to this fact, the study in [66] focuses on the verification of the method consisting in a partial replacement of sulphur with phosphorus atoms, based on calculations of supercells measuring $2 \times 2 \times 2$ and containing 64 atoms.

Figure 8 presents a set of three analysed supercells which correspond to the following configurations: (a) $H_3S_{0.875}P_{0.125}$, (b) $H_3S_{0.5}P_{0.5}$ and (c) $H_3S_{0.375}P_{0.625}$. For each presented cell,

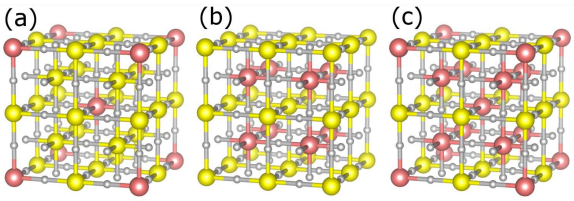

Fig. 8. Supercells formed by doubling an elementary 8-atom cell in each direction. Grey balls represent hydrogen atoms, yellow ones stand for sulphur atoms and red ones correspond to phosphorus atoms [66].

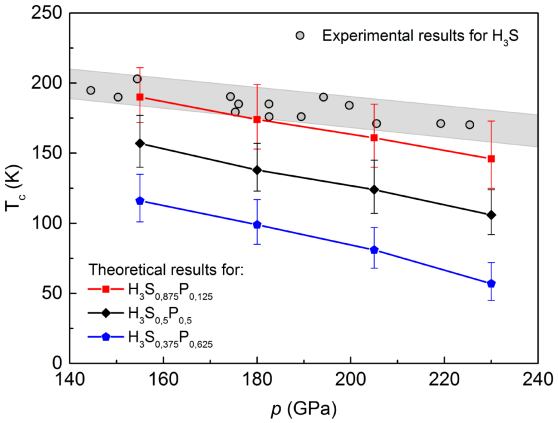

Fig. 9. Critical temperature in the function of pressure for $H_3S_{1-x}P_x$ [66].

there were performed calculations of electronic and phonon structure, and electron–phonon interaction for the pressure of 155, 180, 205 and 230 GPa. The dynamic stability of the analysed systems was confirmed. Next, critical temperature calculations performed with the use of formalism of the Eliashberg equation for a wide range of the Coulomb pseudopotential, from 0.1 to 0.2, showed that doping the compound of H_3S with phosphorus negatively influences the superconducting state. In particular, one could notice a smaller value of critical temperature in the whole range of the analysed pressure values. Interestingly enough, similarly to the case of the work mentioned before, it was possible to reconstruct a trend observed in the experiment, consisting in the decrease in T_c values accompanied by a pressure growth (Fig. 9). It proves a very big inaccuracy of the VCA method used in the publication [81] to determine superconductivity characteristics. The result obtained in [81] does not lead to the conclusion that a partial replacement of sulphur atoms with phosphorus atoms in an elementary cell of H_3S would allow for achieving superconductivity at the temperature close to room temperature.

When analysing the experimental data, it is not difficult to notice that phosphorus and sulphur, which in their coupling with hydrogen display the highest critical temperature values, are neighbours in the periodic table of elements (elements of

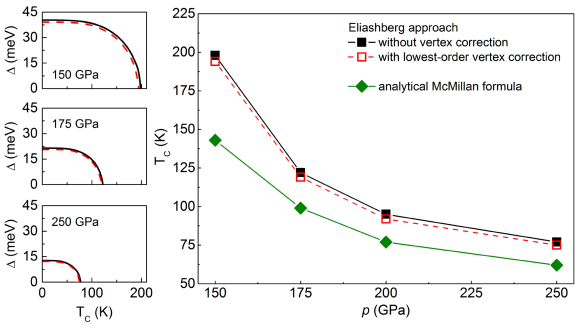

Fig. 10. Order parameter in the temperature function and critical temperature in the function of pressure for H_3Cl [67].

the third period, group VA and VIA). Taking this into account, it may be assumed that also the compound of chlorine and hydrogen might display superconductivity properties (chlorine — an element of the third period, group VIIA), so in [67], the system of H_3Cl has been analysed. One more hypothesis also seems correct. It says that as electronegativity of an element X in the cell H_3X grows, also critical temperature of the system rises [82]. Chlorine, sulphur's neighbour, shows higher electronegativity than phosphorus and sulphur, thus, it is a potential candidate for analysis. Considering the facts above, a complete calculating procedure was performed, which consisted in finding a potential crystal structure for which the enthalpy of the system H_3Cl reaches the lowest value, in determining electron and phonon properties and in determining constant values for the electron–phonon interaction for pressure values from 150 to 250 GPa. It has been shown that for the compound H_3Cl, the structure $Im\bar{3}m$ is the most advantageous energetically and dynamically stable in the pressure range analysed. What is more, it allows for a transition into superconductivity characterized by very strong electron–phonon coupling $\lambda = 2.21$ at the pressure of 150 GPa. Subsequently, a pressure growth makes the value of λ drop to 0.91 for $p = 250$ GPa. On the basis of the determined spectral functions, the critical temperature for H_3Cl was determined alongside with the use of the classic Eliashberg equations and their extended versions, enriched with lowest-order vertex corrections. Additionally, the results obtained were compared with the results calculated with the help of the analytical McMillan formula [83]. Due to a lack of any experimental data, the above mentioned calculations were performed with the assumption of a constant value of the Coulomb pseudopotential ($\mu^\star = 0.13$). This made it possible to determine the influence of vertex corrections on T_c. It turns out that for a fixed value of $\mu^\star$, vertex corrections only slightly reduce the value of critical temperature and band gap.

As Fig. 10 shows, pressure has a significant influence on the order parameter and on T_c as it makes a critical temperature drop from 198 to 77 K in the range of 150 to 250 GPa. Thus, the highest obtained result is close to the record value of critical temperature, experimentally observed in H_3S and may constitute a departure point for further high-pressure experimental measurements. Additionally, the paper tackles the issue of the isotope effect which clearly confirms the classic pairing mechanism in the system of H_3Cl, provided it is experimentally verified.

4. Superconductivity in lanthanum hydrides compounds

The latest discovery in the research of hydrogen-rich compounds that can be considered as groundbreaking was an experimental confirmation of superconductivity in the LaH_{10} compound with T_c exceeding 250 K [84]. In particular, it has been shown that in the LaH_{10} compound the critical temperature of the superconducting state strongly depends on pressure and reaches: $T_c^a = 215$ K and $T_c^b = 260$ K for $p_a = 150$ GPa and $p_b \in (180\text{–}200)$ GPa, respectively. Such promising results became an impulse for further investigations of lanthanum hydrides.

The high-pressure phase stability and superconductivity of lanthanum hydrides LaH_m was explored in [85]. In particular, a number of LaH_m phases ($m = 4, \ldots, 9, 11$) at different pressures was found. Calculation of the critical temperature for all these cases in the required pressure range by using *ab initio* method or a numerical solution of the Eliashberg equations would be very time consuming. Therefore, the A–D formula has been used [86]. This approach allows to calculate — easily and with a fairly good approximation — the value of the critical temperature, as seen in Fig. 11. One can notice there that LaH_{10} shows the highest value of T_c of all considered cases and thus, a more accurate analysis of LaH_{10} is required, namely, the Eliashberg formalism and superconducting density field theory

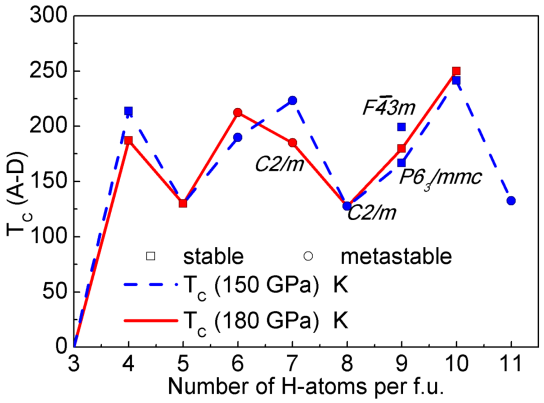

Fig. 11. Superconducting temperatures T_c, obtained using the A–D formula with $\mu^\star = 0.1$ for a series of lanthanum hydrides at 150 and 180 GPa [85].

(SCDFT) [85]. In fact, our results agree with the results achieved by Drozdov et al. [87] which can be related to the introduction of the superconducting phase in the $R\bar{3}m$ structure ($T_c = 206$–223 K). Other experimental results reported in [88] should be related to the superconducting state which is induced in the $Fm\bar{3}m$ structure where supposingly the value of the critical temperature reaches even 280 K. It is worth to mention that previously unknown polyhydride $P6/mmm$ — LaH_{16} was analyzed in [85] indicating a superconductor with T_c of up to 156 K and the superconducting gap of 30 meV at 200 GPa. This means that the addition of further hydrogen atoms does not improve the properties of the superconducting state in that case.

Taking into account the structure of the Eliashberg function for hydrogenated compounds, one can find clearly separated parts coming from hydrogen and the heavy elements which is caused by a huge difference between atomic masses of hydrogen and those elements. Therefore, the addition of a lighter element, like scandium or yttrium atoms, could fill the gap in the Eliashberg function which would mean increasing the electron–phonon coupling and, as a consequence, significantly increasing the value of critical temperature. Applying the above reasoning in [89], it has been shown that the expected range of the critical temperature values for the LaScH and LaYH compounds can reach room temperature. There were taken into account two pressure values: $p_a = 150$ GPa and $p_b = 190$ GPa and for LaScH the results were as follows: $T_c^a \in \langle 220, 267\rangle$ K and $T_c^b \in \langle 263, 294\rangle$ K, while for LaYH there were: $T_c^a \in \langle 218, 247\rangle$ K and $T_c^b \in \langle 261, 274\rangle$ K. It should be noted that the mentioned results were obtained by using the A–D formula and should be confirmed by advanced DFT calculations. Despite this, it provides a good basis for further search of high-temperature superconductors.

5. Summary

Finally, it should be clearly emphasised that the topic concerning hydrogenated compounds is still open. Intensive research carried out in many leading scientific centres all over the world aims not only at increasing critical temperature but also at decreasing external pressure required for metallization and transition into a superconducting state. This may ensure the practical use of such superconductors in the future. One of the possible ways to achieve that might be increasing the concentration of hydrogen atoms in the elementary cell. There are many hopes concerning the systems analysed in the last years in which one heavy atom matches six or ten hydrogen atoms. In particular, the following compounds should be mentioned: CaH_6 ($T_c = 235$ K) [16], YH_6 ($T_c = 247$ K) [36], MgH_6 ($T_c = 270$ K) [90] and YH_{10} ($T_c = 291$ K) [36]. As far, we have theoretical predictions only. Lack of experimental verification hinders further progress in analysing these superconductors. Another way to rise the value of critical temperature could be increasing electron–phonon coupling by adding atoms of the appropriate elements like in the case of lanthanum hydrides compounds. Taking into account a relatively short time since the experimental confirmation of superconductivity in LaH_{10}, next discoveries related to this superconductor can be expected soon.

Acknowledgments

A.P. Durajski acknowledges the financial support from the Polish National Science Centre (NCN) under Grant No. 2016/23/D/ST3/02109.

References

[1] J. Bardeen, L.N. Cooper, J.R. Schrieffer, *Phys. Rev.* **106**, 162 (1957).

[2] J. Bardeen, L.N. Cooper, J.R. Schrieffer, *Phys. Rev.* **108**, 1175 (1957).

[3] J.G. Bednorz, K.A. Müller, *Z. Phys. B* **64**, 189 (1986).

[4] J. Spałek, *Introduction to Condensed Matter Physics*, PWN, 2015 (in Polish).

[5] A. Szewczyk, A. Wiśniewski, R. Puźniak, H. Szymczak *Magnetism and Superconductivity*, PWN, 2012 (in Polish).

[6] N.W. Ashcroft, *Phys. Rev. Lett.* **21**, 1748 (1968).

[7] J.M. McMahon, D.M. Ceperley, *Phys. Rev. B* **84**, 144515 (2011).

[8] R. Szczesniak, M.W. Jarosik, *Solid State Commun.* **149**, 2053 (2009).

[9] E. Maksimov, D. Savrasov, *Solid State Commun.* **119**, 569 (2001).

[10] Y. Yan, J. Gong, Y. Liu, *Phys. Lett. A* **375**, 1264 (2011).

[11] A.P. Durajski, R. Szczesniak, A.M. Duda, *Solid State Commun.* **195**, 55 (2014).

[12] R.P. Dias, I.F. Silvera, *Science* **355**, 715 (2017).

[13] X.-D. Liu, P. Dalladay-Simpson, R.T. Howie, B. Li, E. Gregoryanz, *Science* **357**, (2017).

[14] A.F. Goncharov, V.V. Struzhkin, *Science* **357**, (2017).

[15] N.W. Ashcroft, *Phys. Rev. Lett.* **92**, 187002 (2004).

[16] H. Wang, J.S. Tse, K. Tanaka, T. Iitaka, Y. Ma, *Proc. Natl. Acad. Sci. U.S.A.* **109**, 6463 (2012).

[17] Y. Li, J. Hao, H. Liu, Y. Li, Y. Ma, *J. Chem. Phys.* **140**, 174712 (2014).

[18] Y. Li, G. Gao, Y. Xie, Y. Ma, T. Cui, G. Zou, *Proc. Natl. Acad. Sci. U.S.A.* **107**, 15708 (2010).

[19] G. Zhong, C. Zhang, X. Chen, Y. Li, R. Zhang, H. Lin, *J. Phys. Chem. C* **116**, 5225 (2012).

[20] D. Duan, Y. Liu, F. Tian, D. Li, X. Huang, Z. Zhao, H. Yu, B. Liu, W. Tian, T. Cui, *Sci. Rep.* **4**, 6968 (2014).

[21] S. Endo, A. Honda, S. Sasaki, H. Shimizu, O. Shimomura, T. Kikegawa, *Phys. Rev. B* **54**, R717 (1996).

[22] H. Fujihisa, H. Yamawaki, M. Sakashita, K. Aoki, S. Sasaki, H. Shimizu, *Phys. Rev. B* **57**, 2651 (1998).

[23] R. Rousseau, M. Boero, M. Bernasconi, M. Parrinello, K. Terakura, *Phys. Rev. Lett.* **85**, 1254 (2000).

[24] M. Sakashita, H. Fujihisa, H. Yamawaki, K. Aoki, *J. Phys. Chem. A* **104**, 8838 (2000).

[25] H. Fujihisa, H. Yamawaki, M. Sakashita, A. Nakayama, T. Yamada, K. Aoki, *Phys. Rev. B* **69**, 214102 (2004).

[26] M. Sakashita, H. Yamawaki, H. Fujihisa, K. Aoki, S. Sasaki, H. Shimizu, *Phys. Rev. Lett.* **79**, 1082 (1997).

[27] A.P. Drozdov, M.I. Eremets, I.A. Troyan, arXiv:1412.0460 (2014).

[28] A.P. Drozdov, M.I. Eremets, I.A. Troyan, V. Ksenofontov, S.I. Shylin, *Nature* **525**, 73 (2015).

[29] M. Einaga, M. Sakata, T. Ishikawa, K. Shimizu, M.I. Eremets, A.P. Drozdov, I.A. Troyan, N. Hirao, Y. Ohishi, *Nat. Phys.* **12**, 835 (2016).

[30] N. Bernstein, C. Hellberg, M. Johannes, I. Mazin, M.J. Mehl, *Phys. Rev. B* **91**, 060511 (2015).

[31] Y. Li, L. Wang, H. Liu et al., *Phys. Rev. B* **93**, 020103 (2016).

[32] D. Duan, X. Huang, F. Tian, D. Li, H. Yu, Y. Liu, Y. Ma, B. Liu, T.Cui, *Phys. Rev. B* **91**, 180502 (2015).

[33] H. Fröhlich, *Phys. Rev.* **79**, 845 (1950).

[34] H. Fröhlich, *Proc. R. Soc. A* **223**, 296 (1954).

[35] W. Sano, T. Koretsune, T. Tadano, R. Akashi, R. Arita, *Phys. Rev. B* **93**, 094525 (2016).

[36] K. Tanaka, J.S. Tse, H. Liu, *Phys. Rev. B* **96**, 100502 (2017).

[37] F. Peng, Y. Sun, C.J. Pickard, R.J. Needs, Q. Wu, Y. Ma, *Phys. Rev. Lett.* **119**, 107001 (2017).

[38] G.M. Eliashberg, *J. Exp. Theor. Phys.* **11**, 696 (1960).

[39] J.P. Carbotte, *Rev. Mod. Phys.* **62**, 1027 (1990).

[40] J.P. Carbotte, C. Jiang, *Phys. Rev. B* **48**, 4231 (1993).

[41] H. Chi, J.P. Carbotte, *Phys. Rev. B* **49**, 6143 (1994).

[42] Y. Nambu, *Phys. Rev.* **117**, 648 (1960).

[43] A.L. Fetter, J.D. Walecka, *Quantum Theory of Systems of Many Particles*, PWN, 1982 (in Polish).

[44] W. Gasser, E. Heiner, K. Elk, *Green Functions in Solid-State and Many-Particles Physics*, Wiley-VCH, Berlin 2001 (in German).

[45] G.A.C. Ummarino, in: *Emergent Phenomena in Correlated Matter*, Eds. E. Pavarini, E. Koch, U. Schollwöck, Forschungszentrum Jülich GmbH Verlag, 2013.

[46] F. Marsiglio, J. Carbotte, *Electron-Phonon Superconductivity*, in: *Conventional and Unconventional Superconductors*, Vol. I, Eds. K.H. Bennemann, J.B. Ketterson, Springer-Verlag, Berlin 2008.

[47] P. Giannozzi, S. Baroni, N. Bonini et al., *J. Phys. Condens. Matter* **21**, 395502 (2009).

[48] P. Giannozzi, O. Andreussi, T. Brumme et al., *J. Phys. Condens. Matter* **29**, 465901 (2017).

[49] F. Giustino, M.L. Cohen, S.G. Louie, *Phys. Rev. B* **76**, 165108 (2007).

[50] O.V. Dolgov, R.S. Gonnelli, G.A. Ummarino, A.A. Golubov, S.V. Shulga, J. Kortus, *Phys. Rev. B* **68**, 132503 (2003).

[51] M. Schackert, T. Märkl, J. Jandke, M. Hölzer, S. Ostanin, E.K.U. Gross, A. Ernst, W. Wulfhekel, *Phys. Rev. Lett.* **114**, 047002 (2015).

[52] J. Shi S.-J. Tang, B. Wu et al., *Phys. Rev. Lett.* **92**, 186401 (2014).

[53] S.K. Bose, J. Kortus, *Electron–Phonon Coupling in Metallic Solids from Density Functional Theory* in: *Vibronic and Electron–Phonon Interactions and Their Role in Modern Chemistry and Physics*, Ed. T. Kato, Transworld Research Network, India 2009, p. 1.

[54] P. Morel, P.W. Anderson, *Phys. Rev.* **125**, 1263 (1962).

[55] Y. Yao J.S. Tse, K. Tanaka, F. Marsiglio, Y. Ma, *Phys. Rev. B* **79**, 054524 (2009).

[56] A. Durajski, *Sci. Rep.* **6**, 38570 (2016).

[57] R. Szczesniak, M.W. Jarosik, D. Szczesniak, *Physica B* **405**, 4897 (2010).

[58] J. Bauer, J.E. Han, O. Gunnarsson, *J. Phys. Condens. Matter* **24**, 492202 (2012).

[59] M. Kostrzewa, R. Szczęśniak, J.K. Kalaga, I.A. Wrona *Sci. Rep.* **8**, 11957 (2018).

[60] R. Szczesniak, *Acta Phys. Pol. A* **109**, 179 (2006).

[61] F. Marsiglio, M. Schossmann, J.P. Carbotte, *Phys. Rev. B* **37**, 4965 (1988).

[62] A.P. Durajski, R. Szczesniak, Y. Li, *Physica C* **515**, 1 (2015).

[63] A.P. Durajski, R. Szczesniak, M.W. Jarosik, *Phase Transit.* **85**, 727 (2012).

[64] A. Durajski, R. Szczesniak, *Sci. Rep.* **7**, 4473 (2017).

[65] R. Szczesniak, A. Durajski, *Sci. Rep.* **8**, 6037 (2018).

[66] A. Durajski, R. Szczesniak, *Physica C* **554**, 38 (2018).

[67] A.P. Durajski, R. Szczesniak, *J. Chem. Phys.* **149**, 074101 (2018).

[68] A.P. Durajski, R. Szczesniak, L. Pietronero, *Ann. Phys. (Berlin)* **528**, 358 (2016).

[69] R. Akashi, M. Kawamura, S. Tsuneyuki, Y. Nomura, R. Arita, *Phys. Rev. B* **91**, 224513 (2015).

[70] R. Gonczarek, M. Gładysiewicz-Kudrawiec, *Van Hove's Scenario in High-Temperature Superconductivity*, Oficyna Wydawnicza Politechniki Wrocławskiej, Wrocław 2004 (in Polish).

[71] A.P. Drozdov, M.I. Eremets, I.A. Troyan, arXiv:1508.06224 (2015).

[72] P. Miller, J.K. Freericks, E.J. Nicol, *Phys. Rev. B* **58**, 14498 (1998).

[73] J.K. Freericks, E.J. Nicol, A.Y. Liu, A.A. Quong, *Phys. Rev. B* **55**, 11651 (1997).

[74] I. Errea, M. Calandra, C.J. Pickard, J. Nelson, R.J. Needs, Y. Li, H. Liu, Y. Zhang, Y. Ma, F. Mauri, *Phys. Rev. Lett.* **114**, 157004 (2015).

[75] M. Sakata, Y. Nakamoto, K. Shimizu, T. Matsuoka, Y. Ohishi, *Phys. Rev. B* **83**, 220512 (2011).

[76] J.M. McMahon, D.M. Ceperley, *Phys. Rev. B* **84**, 144515 (2011).

[77] T. Matsuoka, M. Sakata, Y. Nakamoto, K. Takahama, K. Ichimaru, K. Mukai, K. Ohta, N. Hirao, Y. Ohishi, K. Shimizu, *Phys. Rev. B* **89**, 144103 (2014).

[78] C. Buzea, T. Yamashita, *Supercond. Sci. Technol.* **14**, R115 (2001).

[79] Y. Quan, W.E. Pickett, *Phys. Rev. B* **93**, 104526 (2016).

[80] L. Ortenzi, E. Cappelluti, L. Pietronero, *Quantum Stud. Math. Found.* **5**, 35 (2018).

[81] Y. Ge, F. Zhang, Y. Yao, *Phys. Rev. B* **93**, 224513 (2016).

[82] C. Heil, L. Boeri, *Phys. Rev. B* **92**, 060508 (2015).

[83] W.L. McMillan, *Phys. Rev.* **167**, 331 (1968).

[84] A. P. Drozdov, P.P. Kong, V.S. Minkov et al., arXiv:1812.01561 (2018).

[85] I. Kruglov, D.V. Semenok, H. Song, *Phys. Rev. B* **101**, 024508 (2020).

[86] P.B. Allen, R.C. Dynes, *Phys. Rev. B* **12**, 905 (1975).

[87] A.P. Drozdov, V.S. Minkov, S.P. Besedin, P. Kong, M.A. Kuzovnikov, D. Knyazev, M. Eremets, arXiv:1808.07039 (2018).

[88] M. Somayazulu, M. Ahart, A.K. Mishra, Z.M. Geballe, M. Baldini, Y. Meng, V.V. Struzhkin, R.J. Hemley, *Phys. Rev. Lett.* **122**, 027001 (2019).

[89] M. Kostrzewa, K.M. Szczęśniak, A.P. Durajski, R. Szczęśniak, *Sci. Rep.* **10** 1592 (2020).

[90] X. Feng, J. Zhang, G. Gao, H. Liu, H. Wang, *RSC Adv.* **5**, 59292 (2015).